

Rényi Divergence Deep Mutual Learning

Weipeng Fuzzy Huang* Junjie Tao† Changbo Deng* Ming Fan† Wenqiang Wan*
 Qi Xiong* Guangyuan Piao‡

Abstract

This paper revisits an incredibly simple yet exceedingly effective computing paradigm, Deep Mutual Learning (DML). We observe that the effectiveness correlates highly to its excellent generalization quality. In the paper, we interpret the performance improvement with DML from a novel perspective that it is roughly an approximate Bayesian posterior sampling procedure. This also establishes the foundation for applying the Rényi divergence to improve the original DML, as it brings in the variance control of the prior (in the context of DML). Therefore, we propose Rényi Divergence Deep Mutual Learning (RDML). Our empirical results represent the advantage of the marriage of DML and the Rényi divergence. The flexible control imposed by the Rényi divergence is able to further improve DML to learn better generalized models.

1 Introduction

A compelling virtue of certain machine learning techniques is that they show strong connections to realworld phenomena. One member among these techniques is Deep Mutual Learning (DML). It is an empirically very powerful computing paradigm even though it is conceptually simple [34]. The metaphor for DML is simply that, the learning procedure organizes a class of students to learn knowledge not only from the ground truth, but also from their peers. Intuitively, this learning paradigm encourages the students to learn others' strengths. The students therefore perform better than learning knowledge only from the teacher. A possible reason is that this paradigm protects the students from pushing their understanding of certain knowledge to an extreme, as the peers' knowledge can regulate the extreme understanding. After all, DML is a fine paradigm, as that simplicity is better than complexity—as suggested by Occam's razor.

Interestingly, even when each student uses the same network architecture (but with distinct weight initializations), each single model still benefits from the paradigm and outperforms itself [34]. This is reasonable as initialization plays a crucial role in Deep Learning (DL) optimizations because some initial points can lead to wider optima than others, in the highly non-convex optimization tasks [3]. As regards of pretrained models, the dropout mechanism randomly dropping a proportion of parameter values [25] maintains the diversity. In other words, we are able to generate sufficient diversity among a number of instances of the identical architectures, in most cases.

Despite the empirical efficiency, the question for why DML really works remains open to discussion. One way to look at this paradigm is from the perspective of Knowledge Distillation (KD). In fact, KD is a methodology designed for distilling knowledge from an ensemble of large fine trained networks into a smaller network so that the small network can obtain a close performance but be more computationally efficient [9]. DML is an online KD method where every model starts from the same stage (with diverse weight initializations) and shares knowledge from the very beginning [6]. Neither offline nor online KD has been analyzed with a thorough theoretical study. The work [20] provided a preliminary theoretical justification on KD; however, it is limited to basic linear models. Nonetheless, this is expected as DL is inherently challenging for theoretical analysis.

DML is remarkable in constraining the generalization errors and hence nicely protects the learned models from overfitting [18]. Heuristically, it helps the students find wider local optima [34], since the students share diversity with others and avoid being optimized in only very few directions. In this paper, we interpret that DML is approximately equivalent to the process of a Bayesian posterior sampling. Bayesian posterior sampling supports good generalization, since it focuses on the posterior distribution (i.e., the distribution of the model parameters) rather than estimating the parameters via *Maximum Likelihood Estimation* approach. This implies that a good amount of uncertainty is well main-

*Security Big Data Lab, Tencent Inc., China. {fuzzyhuang, changbodeng, johnnywan, keonxiong}@tencent.com

†School of Software Engineering, Xi'an Jiaotong University, China. taojunjie@stu.xjtu.edu.cn, mingfan@mail.xjtu.edu.cn

‡Department of Computer Science, Maynooth University, Ireland. guangyuan.piao@mu.ie

tained in the entire model. On top of this observation, we propose to replace the Kullback–Leibler (KL) divergence for learning the differences from others by the Rényi divergence [4], which can be thought of as a super-class of KL divergence. It allows us to further tune the variance of the priors approximated by DML. Finally, we coin this paradigm Rényi Divergence Deep Mutual Learning (RDML).

Our contributions are summarized here. We connect the DML and the Rényi divergence to the Bayesian learning for interpreting their working machinery in Section 4. In the same section, we propose to replace the KL divergence by the Rényi divergence which is more controllable and tunable to further improve the model performance. Moreover, we empirically show that the Rényi divergence can further improve the model performance and achieve better generalizations in Section 5. Finally, the codebase is available at <http://github.com/parklize/rdml>.

2 Related Work

In this section, we review related work, with emphasis on DML and the Rényi divergence.

DML is one of the main knowledge distillation schemes which distill knowledge from a deep neural network into another network. In contrast to offline distillation in which knowledge is transferred from a pre-trained model into another model, DML allows multiple neural networks to transfer knowledge in a collaborative manner during the training process and provides flexibility to train different networks as well as the same networks [6]. Due to its effectiveness, DML has been used in a wide variety of contexts and applications such as tracking visual objects [35], machine translation [36], speech recognition [15], and COVID19 recognition [31]. For example, MutualNet [30] has been proposed to train a cohort of sub-(convolutional) networks with different configurations of network widths and input resolutions via DML to achieve adaptive accuracy-efficiency tradeoffs. Park et al. [18] have extended and applied DML in the context of deep metric learning beyond classification tasks and showed the effectiveness of DML over individual models.

The Rényi divergence [4] has drawn growing attention for the community and has been employed to more applications. For instance, the Rényi divergence has been employed to replace KL divergence in variational inference [13] wherein examples show that the Rényi divergence can control the regularization power of the inferred variational distribution. There are also a number of related applications in cryptography [1, 21] as the Rényi divergence is able to provide tighter security bounds. Recently, the Rényi divergence is also applicable in analyzing human beings’ brain behaviors [23].

These have illustrated the potential of this divergence in a broad range of tasks. Our work proposes to employ the Rényi divergence instead of KL divergence in the DML framework to achieve improvements through greater flexibility.

3 Deep Mutual Learning

Before proceeding to explain the frameworks, we first introduce the common notation which will be consistent throughout the paper. Considering a data size N , let us define the collection of data $\mathcal{D} = \{(x_n, y_n)\}_{1 \leq n \leq N}$ where x_n is the n th datum and y_n is the corresponding ground truth. In addition, we write $\mathbf{x} = \{x_n\}_{1 \leq n \leq N}$ and $\mathbf{y} = \{y_n\}_{1 \leq n \leq N}$. Let $\mathbb{KL}(\cdot)$ denote the KL divergence and $D_\alpha(\cdot)$ denote the Rényi divergence. If an arbitrary random variable X is distributed by distribution $p(X)$, it is written as $X \sim p(X)$. Furthermore, \simeq reads “be approximately equivalent to”. Meanwhile, we denote by θ the model parameters in any generic model. Let K be the number of models in the DML paradigm. Finally, let β denote the learning rate in the optimization techniques.

In the remainder of the section, we first introduce the vanilla DML framework and later demonstrate the DML with the Rényi divergence.

3.1 Vanilla DML Imagine that there are a cohort of students learning a task together. It consists of a base loss and a divergence loss for every single student. Specifically, the DML loss \mathcal{L}_{dml}^k for student k is defined by

$$(3.1) \quad \mathcal{L}_{dml}^k := \mathcal{L}_{base}^k + \mathcal{L}_{div}^k,$$

where \mathcal{L}_{base}^k is the loss objective of the input data and the ground truth, and \mathcal{L}_{div}^k is the divergence loss from this student to others. In general, the base loss is selected depending on the task and the data, e.g., a cross entropy for classification. For example, in a multiclass classification task containing M classes, the base loss is

$$(3.2) \quad \mathcal{L}_{base}^k(\mathbf{y}; \mathbf{x}) = -\frac{1}{N} \sum_{n=1}^N \sum_{m=1}^M \mathbb{1}(y_n = m) \log p_{nm}^{(k)}$$

where $p_{nm}^{(k)}$ denotes the probability of the n th datum belonging to class m with regard to model k ¹.

The divergence loss \mathcal{L}_{div}^k is based on the predictive probability distribution P^k for each student k . In the vanilla DML, the KL divergence is applied to compute the distance from P^k to $P^{k'}$ such that

$$(3.3) \quad \mathcal{L}_{div}^k = \frac{1}{K-1} \sum_{k' \neq k} \mathbb{KL}(P^{k'} \parallel P^k),$$

¹We use “(k)” instead of “ k ” in the superscript for the index of model when there is confusion between exponent and itself

Algorithm 1 LEARNING PROCEDURE OF DML

```

1:  $\theta_k$ : the parameters for student  $k$ 
2: while not converged do
3:   for  $k = 1, \dots, K$  do
4:      $\theta_k \leftarrow \theta_k - \beta \nabla_{\theta_k} \mathcal{L}_{dml}^k$ 

```

which indicates that the model k will be calibrated by other models. Concerning the formalism defined above, the learning process is sketched in Algorithm 1. It iterates through each student and optimizes the parameters upon the corresponding DML loss. Although we exemplify it using classification, we emphasize that this framework can be trivially extended to a diversity of machine learning tasks.

3.2 DML with the Rényi Divergence The Rényi divergence, as a superclass of the KL divergence, introduces more flexibility of managing the divergence value. In DML, it facilitates the control of the degree of effort that one student should spend on learning from others. We propose to replace the KL divergence in \mathcal{L}_{div}^k in DML to acquire a more controllable computation paradigm, which we name RDML. Next, we discuss on the Rényi divergence.

3.2.1 Rényi divergence The divergence is a statistical distance quantity with a controlling parameter $\alpha \in [0, 1) \cup (1, \infty)$ and thus is also called α -divergence. It measures the distribution distance from Q to P , which is defined by

$$(3.4) \quad D_\alpha(P||Q) = \frac{1}{\alpha - 1} \log \int p(\mu)^\alpha q(\mu)^{1-\alpha} d\mu.$$

Setting $\alpha = 1$ is invalid according to the above definition. Same as the KL divergence, the Rényi divergence is asymmetric and hence is in general not a metric [4]. The Rényi divergence covers a family of statistical distances. For instance, $\alpha = 0.5$ leads the Rényi divergence to the squared Hellinger divergence and $\alpha \rightarrow 1$ leads to the KL divergence, etc. [13].

Furthermore, the following essential remarks have been proved in [4] (however, we still provide two simpler proofs in the supplemental material for a quick verification of these two facts).

REMARK 1. For any distribution P , Q , and $\alpha \in [0, 1) \cup (1, \infty)$, the Rényi divergence $D_\alpha(P||Q) \geq 0$. The equality holds if and only if $P \equiv Q$.

REMARK 2. Given $\alpha \in [0, 1) \cup (1, \infty)$, the Rényi divergence $D_\alpha(P||Q)$ is non-decreasing in α , for any distribution P and Q .

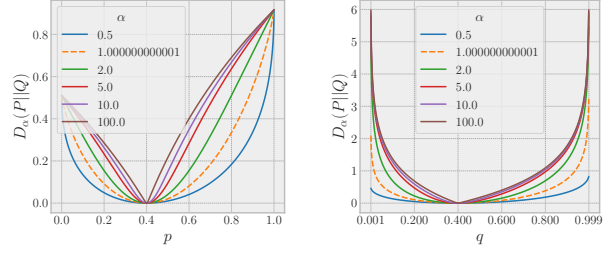


Figure 1: Example plots of the Rényi divergence for distributions containing two events. The orange dashed line is for the KL divergence in both plots. The first plot fixes distribution Q to $(0.4, 0.6)$ and shows the divergence change over p and $1 - p$. The second plot fixes $P = (0.4, 0.6)$ and shows the divergence change over q and $1 - q$. Note that, either $q = 0$ or $q = 1$ obtains the divergence value ∞ for all possible α . Since infinity is technically not drawable, the x-axis in the second plot ranges from 0.001 to 0.999.

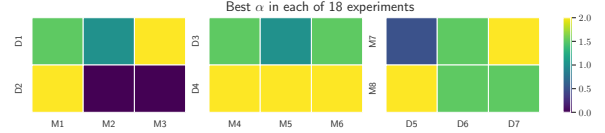


Figure 2: Heatmap of the best α values of 18 experiments in Section 5 where each experiment is a unique combination of a method M and a dataset D . A method with different datasets (and vice versa) will require different α to perform better.

The first remark fixes the lower bound of the divergence. This property ensures \mathcal{L}_{dml} to be non-negative, which is always a desired property for the loss function. Remark 2 indicates that α controls the distance values when P and Q are fixed. In the context of DML, a larger α hence pushes the students to learn more from the peers considering that the gradients for updating the parameters become larger.

Figure 1 illustrates an example of the $D_\alpha(P||Q)$, for various α with fixed P and Q respectively. In the example, the Rényi divergence with $\alpha \rightarrow 1$ is the KL divergence. We observe that the correlation between $D_\alpha(P||Q)$ and α perfectly embodies Remark 2. On the other hand, the case of focusing on $D_\alpha(P||Q)$ with fixed P , spans a much greater range. The divergence is more sensitive for $P \neq Q$ in this scenario with sufficiently large α . That said, the gap between $\alpha = 10$ and $\alpha = 100$ is smaller, which implies that the divergence growth will become much slower as α increases.

As shown, α introduces the flexibility of controlling

the degree any student learns from others in the context of DML. The degree that a student should learn from her peers depends on the situation. This can also be noticed from Figure 2 in which the best α values vary across 18 experiments depending on the method and dataset in each experiment in Section 5. Analogous to those regularized approaches, the model performance always benefits from a better tuned regularization power, i.e., the coefficient for the regularization part.

4 Why DML and the Rényi Divergence Work

In our findings, the major reason for why DML works is that DML better mitigates the overfitting for each single model and thus obtains better generalization for training the models. A general reason for causing overfitting is the ignorance to uncertainty [14]. The advantage of the DML framework lies on its ability to generate good perturbations during the parameter updating phase. Hence, a reasonable amount of uncertainty is incorporated in the training procedure.

In the sequel, we provide a Bayesian interpretation of DML. To keep our interpretation sufficiently precise, we restrict that all students use the same architecture.

4.1 A Bayesian Interpretation of DML and the Rényi Divergence To summarize, a gradient-based parameter updating step in DML is approximately equivalent to Bayesian posterior sampling, even though only a small batch of data is drawn to update the parameters at each timestamp in this sort of approach. The parameter α in the Rényi divergence acts as a control to indirectly manage the prior variance.

Stochastic Gradient Descent (SGD) and its variants are usually not preferred in inferring Bayesian models, as they will converge to the *Maximum a Posteriori* rather than the true posterior. This is partly due to the fact that the parameter set of a Bayesian model is in non-Euclidean geometric space [5]. That being said, SGD still strongly correlates to the Markov Chain Monte Carlo (MCMC) algorithms, the standard approach for inferring the Bayesian models. For example, Stochastic Gradient Langevin Dynamics [28] is a gradient-based method applying the Langevin Dynamics mechanism to inject proper noise to ensure the parameters converge to that of the true posterior. Most recently, Mingard et al. [16] show that with some neural network architectures, the SGD-obtained posterior probability $p_S(\theta|\mathcal{D})$ correlates extraordinarily to the Bayesian-obtained posterior probability $p_B(\theta|\mathcal{D})$, so that SGD can be viewed as a Bayesian sampler in certain circumstances. Interestingly but unsurprisingly, this result also holds with other gradient-based algorithms including Adam, AdaGrad, and RMSprop, etc. [16]. Therefore, noting that

posterior $p(\theta|\mathcal{D})$ follows $p(\theta|\mathcal{D}) \propto p(\theta, \mathcal{D}) = p(\mathcal{D}|\theta)p(\theta)$, we set up the following assumption in order to verify our interpretation later.

ASSUMPTION 1. *When SGD is applied to minimize the negative joint probability of data and parameters, such that $\theta = \theta - \beta \nabla_{\theta}(-\log p(\theta, \mathcal{D})) = \theta + \beta \nabla_{\theta} \log p(\theta, \mathcal{D})$, it is approximately equivalent to (\simeq) that $\theta \sim p(\theta|\mathcal{D})$.*

4.2 Interpreting DML A neural network can considerably be regarded as a blackbox function approximating a hard-to-define distribution. Let us follow [11] to formulate $f(\mathbf{x}, \theta)$ a neural network where θ is the parameter set in the network, where $P = f(\mathbf{x}, \theta)$ are the approximated probabilities for certain tasks. Taking multiclass classification as an example again, we write $p(\mathbf{y}|\mathbf{x}, \theta) = \text{Categorical}(\mathbf{y}; P)$ such that the label assignment \mathbf{y} is thought to be sampled from a categorical distribution upon distribution P . The negative logarithm of this likelihood function is identical to the cross entropy loss, i.e.,

$$(4.5) \quad \mathcal{L}_{base}(\mathbf{y}; P) = -\log p(\mathbf{y}|\mathbf{x}, \theta).$$

Minimizing the base loss is in effect to maximize the log likelihood.

Similar to Bayesian linear regression, \mathbf{x} is the known covariate and thus a constant. If θ is a random variable then $P \sim f(\mathbf{x}, \theta)$, where $P^k = f(\mathbf{x}, \theta_k)$ and θ_k is sampled from a hard-to-define prior $p(\theta)$. In (R)DML, we have

$$\nabla_{\theta_k} \mathcal{L}_{div}^k = \frac{1}{K-1} \sum_{k' \neq k} \nabla_{\theta_k} D_{\alpha}[f(\mathbf{x}, \theta_{k'}) || f(\mathbf{x}, \theta_k)].$$

Considering that \mathbf{x} is constant, the randomness of $f(\mathbf{x}, \theta_k)$ is completely decided by θ . Using a proper learning rate, the minimization step moves θ_k towards every $\theta_{k'}$ with a reasonably small pace, in the probability space. While temporarily ignoring \mathcal{L}_{base}^k , the SGD step related to \mathcal{L}_{div}^k simulates a stochastic process for moving each θ_k reasonably closer to the true mean θ^* (in a non-Euclidean space). The group of θ_k are then random scatters around the true mean θ^* . Hence, we regard $\theta_k \sim p(\theta_k|\theta^*, \eta)$ where η is the parameter for the unknown prior. As the prior is unknown, it is challenging to decide η and therefore an empirical approach for simulating this prior is well suited in the scenario. Hence, omitting the hyperparameter set (θ^*, η) , we obtain

$$(4.6) \quad \nabla_{\theta_k} \mathcal{L}_{div}^k \simeq \nabla_{\theta_k} [-\log p(\theta_k)]$$

as moving towards the prior mean should increase the prior probability $p(\theta_k|\theta^*, \eta)$ in most cases. This approach relies on the empirical information for updating the information in the prior.

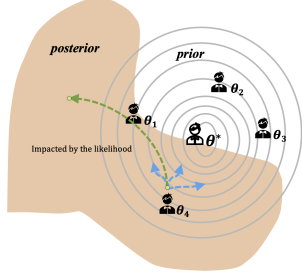


Figure 3: The illustration of θ_k 's movements in DML. Curly arrows are used to emphasize that the movements are nonlinear. In this case, θ_4 approaches the true θ^* by moving towards other peers. Besides its movement towards the true θ^* , its update will still be influenced by the likelihood.

DML considers both the likelihood (Equation (4.5)) and prior part (Equation (4.6)), such that

$$\begin{aligned}\theta_k &= \theta_k - \beta \left(\nabla_{\theta_k} \mathcal{L}_{base}^k + \nabla_{\theta_k} \mathcal{L}_{div}^k \right) \\ &\simeq \theta_k - \beta \nabla_{\theta_k} (-\log p(\mathbf{y}|\mathbf{x}, \theta_k) - \log p(\theta_k)) \\ &= \theta_k + \beta \nabla_{\theta_k} \log p(\mathbf{y}, \mathbf{x}, \theta_k) = \theta_k + \beta \nabla_{\theta_k} \log p(\mathcal{D}, \theta_k)\end{aligned}$$

where the last line comes from that $p(\mathbf{x})$ is constant. According to Assumption 1, we arrive at

$$\theta_k = \theta_k - \beta \nabla_{\theta_k} \mathcal{L}_{dml}^k \simeq \theta_k \sim p(\theta_k|\mathcal{D}).$$

Hence, we reach the conclusion that DML is approximately equivalent to an MCMC posterior sampling for the parameter θ while its prior is defined by an empirical approximation of the unknown prior. Figure 3 depicts an illustrative example of this process.

4.3 Advantage of the Rényi Divergence in DML

Adopting the Rényi divergence in DML incorporates another flexible control to this stochastic process. In other words, α controls the variance of this empirical prior, and a larger α results in smaller variance. Additionally, α imposes nonlinear change to the control of the movement of each θ in the probability space. Given Remark 2, at each timestamp, θ moves in a larger pace to the mean with a greater α , while it can move slower with a smaller α . As pointed out in [14], a prior better explaining the data does not necessarily lead to a better generalized posterior. Thus, we should embrace the flexibility to allow for broader prior choices wherein there is a greater chance to seek a better solution.

4.4 Comparing with DML & Linear Scaling

Alternatively, one may consider multiplying the KL

divergence part in the loss with a linear scale factor $\psi > 0$. Following that, the objective can be written as

$$\begin{aligned}\max_{\theta} \log p(\mathbf{y}|\theta, \mathbf{x}) + \psi \log p(\theta) \\ \equiv \max_{\theta} 1/\psi \log p(\mathbf{y}|\theta, \mathbf{x}) + \log p(\theta).\end{aligned}$$

This implies that the corresponding posterior roughly assumes $p(\theta|\mathcal{D}, \psi) \propto p(\mathbf{y}|\theta, \mathbf{x})^{1/\psi} p(\theta)$. If $0 < 1/\psi \leq 1$ is satisfied, this is namely the *power posterior*, which is proved as a more robust Bayesian posterior [32, 7]. The power posterior provides better performance when the prior is misspecified (in some sense, overfitting). While the prior is sufficiently good, general posteriors will work as well as power posteriors. That is, seeking a nicer prior is still in a higher order. Referring to our situation, it means that this approach and RDML are not competitors and can collaborate with no conflict.

5 Empirical Study

The empirical study aims to explore if RDML is capable of uplifting the model performance more than the vanilla DML and the single models. Hence, we reduce the effort in tuning the models but instead will follow some general settings. We focus on the following research questions.

1. How does RDML perform compared with the vanilla DML and the single model on its own?
2. Does RDML generalize better?

5.1 Setup The tested data covers the two popular fields Computer Vision (CV) and Natural Language Processing (NLP). The CV data contains CIFAR10 and CIFAR100 [12] for resolution 32×32 . We examine on DTD [2] and Flowers102 [17] for resolution 224×224 . These datasets are used to conduct experiments for the image classification task. The NLP data for text classification task contains AGNews, Yahoo!Answers, and YelpReviewFull. All data is handled through either `torchvision`² or `torchtext`³.

Regarding CIFAR10 and CIFAR100, we utilize the SGD with Nesterov momentum 0.9. The initial learning rate is set to 0.1 and the weight decay is set to 0.0005. Apart from that, we run 200 epochs in total for a batch size 128. The learning rate drops by 0.2 at every 60th epoch. In light of the architectures, we adopt GoogLeNet [27], ResNet34 [8], and VGG16 [24]⁴. As regards of DTD and Flowers192, we set the learning

²<https://pytorch.org/vision/stable/datasets.html>

³<https://pytorch.org/text/stable/datasets.html>

⁴The implementations of these three architectures are from <https://github.com/weiaicunzai/pytorch-cifar100>

Table 1: Top-1 accuracy (%) results for CIFAR10 and CIFAR100. For a stabler outcome, we average the accuracy of the test set in the last 10 epochs. Also, the same models are reindexed by their values in an ascending order. In the table, GN is abbreviated for GoogLeNet, RN is short for ResNet34, and VG is short for VGG16. The subscript of a model is the model index, starting from 0. RDML _{α} means that it sets the α value as α . The independent case (Ind.) has only one result.

	Dataset: CIFAR10						Dataset: CIFAR100					
	GN ₀	GN ₁	RN ₀	RN ₁	VG ₀	VG ₁	GN ₀	GN ₁	RN ₀	RN ₁	VG ₀	VG ₁
Ind.	91.87		92.56		90.71		69.61		76.26		72.21	
RDML _{0.5}	91.91	92.06	92.86	93.03	91.03	91.26	70.22	70.24	76.71	77.14	72.09	72.53
DML	92.28	92.37	93.27	93.34	91.22	91.33	72.34	72.49	77.14	77.24	73.01	73.17
RDML _{1.5}	92.61	92.62	93.28	93.35	91.17	91.29	71.65	72.1	77.61	77.94	73.32	73.6
RDML _{2.0}	92.26	92.28	93.18	93.19	91.17	91.23	72.13	72.26	78.31	78.5	73.30	73.74

Table 2: Top-1 accuracy (%) results for DTD and Flowers102. We average the accuracy results of the last 5 epochs in the test set. In the table, IV4 is abbreviated for InceptionV4 and YV3 is short for YoloV3. Ind. is again the independent case and the subscript of RDML is the α value. The same models are reindexed by their values in an ascending order.

	Dataset: DTD						Dataset: Flowers102					
	IV4 ₀	IV4 ₁	ViT ₀	ViT ₁	YV3 ₀	YV3 ₁	IV4 ₀	IV4 ₁	ViT ₀	ViT ₁	YV3 ₀	YV3 ₁
Ind.	64.66		72.55		68.95		85.70		98.23		82.94	
RDML _{0.5}	64.40	65.89	72.77	73.94	69.50	69.89	84.14	84.21	98.28	98.52	78.01	78.47
DML	65.87	66.20	74.41	75.11	69.93	70.23	84.94	85.01	98.23	98.54	78.89	79.25
RDML _{1.5}	67.57	67.67	75.96	76.01	70.90	71.72	83.82	84.11	98.68	99.09	80.03	80.21
RDML _{2.0}	67.86	68.97	75.37	76.12	71.17	71.26	83.53	84.26	98.99	99.01	80.74	81.1

Table 3: Top-1 accuracy (%) results for the test sets of AGNews, Yahoo!Answers, and YelpReviewFull. The best performing α of RDML is chosen based on the mean accuracy of K models on each test set.

Dataset	fastText				CharCNN			
	Independent	fastText-0	fastText-1	α	Independent	CharCNN-0	CharCNN-1	α
AGNews	89.724	89.763	89.763	2.0	87.132	89.632	89.171	1.5
Yahoo!Answers	65.645	65.650	65.650	0.5	63.538	64.542	64.507	2.0
YelpReviewFull	54.262	54.308	54.312	1.5	55.014	55.358	55.582	1.5

rate to 0.005 and set weight decay as 0.0001 using the SGD with momentum 0.9. We run 30 epochs with batch size 32 and decay the learning rate by 0.1 at epochs (16, 22). Also, the gradients are clipped by the max norm 5. For these two datasets, **timm**⁵ is applied to acquire the pretrained weights for the models: InceptionV4 [26], ViT [29], and YoloV3 [22]. In text classification, we examine fastText [10] with GloVe [19] (pretrained word embeddings) and CharCNN [33] using a public implementation⁶. We empirically set an initial learning rate to 0.0001 and set the weight decay to 0.9 for

the experiments with CharCNN for Yahoo!Answers and YelpReviewFull. Apart from that, we use the default settings of the implementation with an initial learning rate to 0.001 and set the weight decay to 0.5 for all other experiments. Finally, 20 epochs are run and the learning rate is decayed every three epochs with a batch size of 128, for each dataset and method.

Although a larger K must be in favor for better approximating the prior, a pragmatic solution has to cope with the runtime efficiency. We follow [34] to set $K = 2$ which suffices to raise the model performance.

5.2 Evaluation This subsection is dedicated to answer the first question.

⁵<https://rwightman.github.io/pytorch-image-models>

⁶[https://github.com/AnubhavGupta3377/](https://github.com/AnubhavGupta3377/Text-Classification-Models-Pytorch)

Text-Classification-Models-Pytorch

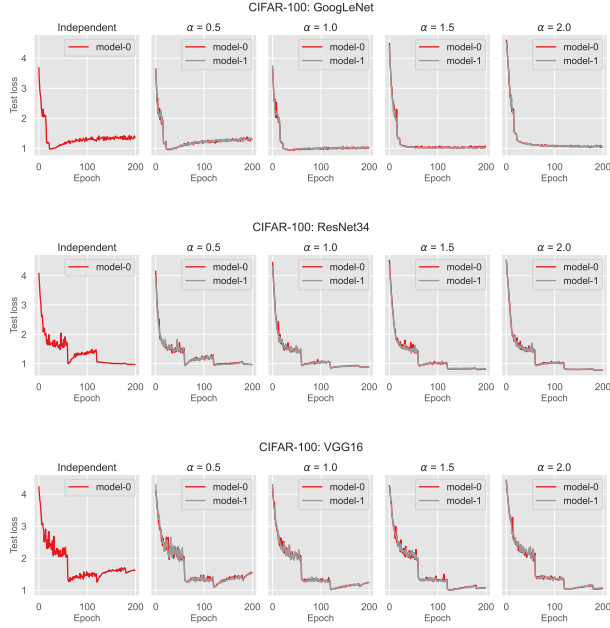


Figure 4: Test loss of RDML for various α on the CIFAR100 dataset

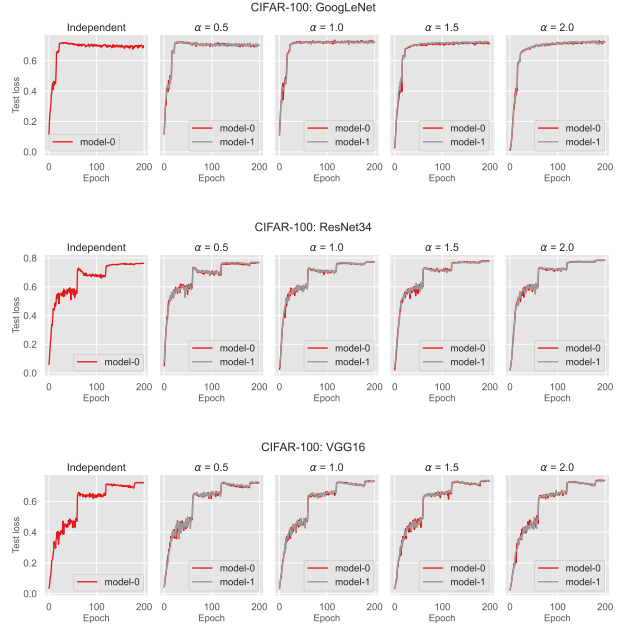


Figure 5: Test accuracy of RDML for various α on the CIFAR100 dataset

Image Classification. The training set and test set are split automatically through **torchvision**. As for classification, we employ the top-1 accuracy to examine the model performance. The experiments are run upon a range of configurations, including the independent case and $\alpha \in \{0.5, 1, 1.5, 2\}$. The results for **CIFAR10** and **CIFAR100** are shown in Table 1, and those for **DTD** and **Flowers102** are displayed in Table 2. The indices of the models are sorted by their values. We label the column-wise best performer using the bold face.

With respect to **CIFAR10**, the results show that for GoogLeNet and ResNet34, RDML with $\alpha = 1.5$ are the winner, while vanilla DML obtains the best accuracy with VGG16. In the experiments for **CIFAR100**, the three selected architectures achieve the best outcomes with $\alpha = 2$ in most cases. Observed from the results, RDML under certain configuration always outperforms the independent case. It demonstrates that tuning α is helpful in learning better model parameters. Regarding **DTD**, $\alpha = 2$ and $\alpha = 1.5$ are still best options for the selected architectures. Same as DML, RDML also perfectly collaborates with the pretrained models which are agreed to be more powerful in modern DL tasks [3]. Additionally, we notice that the improvements over the independent model are greater with these models.

Flowers102 is an interesting case that the performance of InceptionV4 and YoloV3 both downgrade when employing DML or RDML. After investigating more, we notice that this strongly points to generalization and

leave more discussion in Section 5.3.

Text Classification. Similar to the image classification, we adopt the top-1 accuracy for evaluation. Here, we demonstrate α can also be tuned with a grid search on validation set as a hyperparameter. To this end, we choose α based on a grid search $\in \{0.5, 1, 1.5, 2\}$ using a validation set (which is 20% of the training set), and investigate what the best performing α values are and the corresponding performance on the test set. More specifically, the α leading to the highest average accuracy on the test set is presented. The results are summarized in Table 3.

Clearly, the best performing α values vary depending on models and datasets, and improves the independent model consistently, which is in line with the observations of our results on image classification. We also note that, regularization via RDML is more beneficial for the larger models with respect to improving the performance over the corresponding independent model, e.g., CharCNN (with $\sim 2M$ parameters) versus fastText (with $\sim 3K$ parameters). This coincides with the fact that larger models are generally more prone to overfitting and hence RDML is a valuable addition to them.

5.3 Generalization Results In this section, we examine the generalization ability of the RDML over the choice of α , for answering the second research question. We focus on the test performance of **CIFAR100** and **Flowers102**. The other results are placed in the

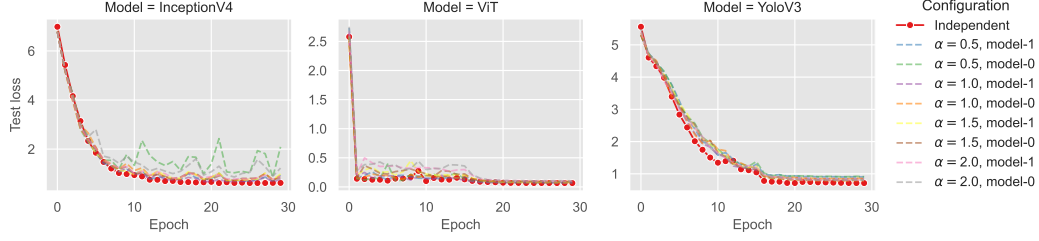


Figure 6: Test loss plots for **Flowers102**

supplemental material.

First of all, we check the base loss for the test data with regard to the **CIFAR100** dataset in Figure 4. It is commonly agreed in the machine learning community that the training loss can be constantly decreased while the test loss will be climbing after a certain point. In Figure 4, the test loss of a single model (either GoogLeNet, ResNet34, or VGG16) perfectly replicates this agreement. However, RDML is able to contain this growth tendency of test loss for all students; and, clearly, the capability of preventing this increase gets enhanced as α becomes larger, i.e. setting a prior with smaller variance. Moreover, we observe that RDML with larger α significantly reduces the fluctuations in the test loss, i.e., the variance is being reduced for the test loss (though it still maintains a reasonable amount of uncertainty). It shows that $\alpha = 2$ for GoogLeNet over-regularizes the model and thus performs slightly worse than that with $\alpha = 1.5$. In the classification problem, the test base loss is the negative likelihood of the unseen data and it can be optimized via RDML. The results indicate that RDML is able to achieve better generalizations through tuning the parameter α .

Similar patterns are observed while checking the test accuracy in Figure 5. In regard to ResNet34, starting from epoch 60, the single model boosts its accuracy since the learning rate is decayed, but rapidly receives a drop in the accuracy. However, it shows that this drop can be significantly mitigated by RDML and achieve the best outcome when $\alpha = 2$ within the range of our choices. Correspondingly, the results for ResNet34 in Figure 4 show a loss increase during the same period. As shown, RDML can limit this loss increasing speed and can limit harder with greater α .

Flowers102. We argue that **Flowers102** is a considerably simpler dataset since all models can easily achieve high test accuracy. Figure 6 depicts that the independent cases of both InceptionV4 and YoloV3 in this task (along with the configuration) have been generalizing very well. The red solid and circled lines, for the independent runs, are clearly distinguishable from others. Though, this generalization does not necessarily help the

model outperform others due to the model capacity but indicates that it may highly exploit its own potential. Since the model on its own has been outstanding in generalization, the uncertainty that RDML brings to the model will be excessive and redundant. For ViT, the solid red line performs nicely in the first 15-16 epochs. However, RDML with $\alpha = 1.5$ and $\alpha = 2$ catch up in the latter epochs. Finally, it excels the independent case but the improvement is not very significant.

5.4 Discussion Through this empirical study, we demonstrate that RDML is able to improve on the vanilla DML and the independent model in most cases. This covers a broad collection of network architectures and datasets. In the selection of our experiments, RDML is shown more valuable when dealing with harder tasks and underperforming configurations, which is also reasonable since a perfect model for a simple task already suffices to reach the maximum performance. Imposing extra components to such a process can ruin its performance.

6 Conclusion

In this paper, we have revisited DML and interpreted it from a Bayesian perspective. Inspired by the interpretation that DML and Rényi divergence are a good combination for learning more generalized models, we propose RDML which is more flexible for further tuning the generalization. The experimental results agree with our findings and demonstrate that RDML has greater capacity than DML for improving the model performance. Last but not least, we expect that our Bayesian interpretation of DML may inspire theorists to conduct more versatile and interesting analysis.

References

- [1] S. Bai, T. Lepoint, A. Roux-Langlois, A. Sakzad, D. Stehlé, and R. Steinfeld, *Improved Security Proofs in Lattice-based Cryptography: Using the Rényi Divergence Rather Than the Statistical Distance*, Journal of Cryptology, 31 (2018), pp. 610–640.

- [2] M. Cimpoi, S. Maji, I. Kokkinos, S. Mohamed, , and A. Vedaldi, *Describing Textures in the Wild*, in CVPR, 2014.
- [3] D. Erhan, A. Courville, Y. Bengio, and P. Vincent, *Why Does Unsupervised Pre-training Help Deep Learning?*, JMLR, (2010), pp. 201–208.
- [4] T. V. Erven and P. Harremoës, *Rényi Divergence and Kullback-Leibler Divergence*, IEEE Transactions on Information Theory, 60 (2014), pp. 3797–3820.
- [5] M. Girolami and B. Calderhead, *Riemann Manifold Langevin and Hamiltonian Monte Carlo methods*, Journal of the Royal Statistical Society: Series B (Statistical Methodology), 73 (2011), pp. 123–214.
- [6] J. Gou, B. Yu, S. J. Maybank, and D. Tao, *Knowledge Distillation: A Survey*, ICCV, 129 (2021), pp. 1789–1819.
- [7] P. Grünwald, *The Safe Bayesian: Learning the Learning Rate via the Mixability Gap*, Lecture Notes in Computer Science, 7568 LNAI (2012), pp. 169–183.
- [8] K. He, X. Zhang, S. Ren, and J. Sun, *Deep Residual Learning for Image Recognition*, in CVPR, 2016, pp. 770–778.
- [9] G. Hinton, O. Vinyals, and J. Dean, *Distilling the Knowledge in A Neural Network*, arXiv preprint arXiv:1503.02531, 2 (2015).
- [10] A. Joulin, E. Grave, P. Bojanowski, and T. Mikolov, *Bag of tricks for efficient text classification*, arXiv preprint arXiv:1607.01759, (2016).
- [11] D. P. Kingma and M. Welling, *An Introduction to Variational Autoencoders*, Foundations and Trends® in Machine Learning, 12 (2019), pp. 307–392.
- [12] A. Krizhevsky and G. Hinton, *Learning multiple layers of features from tiny images*, (2009).
- [13] Y. Li and R. E. Turner, *Rényi Divergence Variational Inference*, NeurIPS, 29 (2016).
- [14] S. Lotfi, P. Izmailov, G. Benton, M. Goldblum, and A. G. Wilson, *Bayesian Model Selection, the Marginal Likelihood, and Generalization*, in ICML, vol. 162, PMLR, 17–23 Jul 2022, pp. 14223–14247.
- [15] R. Masumura, M. Ihori, A. Takashima, T. Tanaka, and T. Ashihara, *End-to-end Automatic Speech Recognition with Deep Mutual Learning*, in APSIPA ASC, IEEE, 2020, pp. 632–637.
- [16] C. Mingard, G. Valle-Pérez, J. Skalse, and A. A. Louis, *Is SGD a Bayesian sampler? Well, almost.*, JMLR, 22 (2021), pp. 1–64.
- [17] M.-E. Nilsback and A. Zisserman, *Automated Flower Classification over a Large Number of Classes*, in Proceedings of the Indian Conference on Computer Vision, Graphics and Image Processing, Dec 2008.
- [18] W. Park, W. Kim, K. You, and M. Cho, *Diversified mutual learning for deep metric learning*, in ECCV, Springer, 2020, pp. 709–725.
- [19] J. Pennington, R. Socher, and C. D. Manning, *Glove: Global vectors for word representation*, in EMNLP, 2014, pp. 1532–1543.
- [20] M. Phuong and C. Lampert, *Towards understanding knowledge distillation*, in ICML, 2019, pp. 5142–5151.
- [21] T. Prest, *Sharper Bounds in Lattice-Based Cryptography using the Rényi Divergence*, in International Conference on the Theory and Application of Cryptology and Information Security, 2017, pp. 347–374.
- [22] J. Redmon and A. Farhadi, *Yolov3: An incremental improvement*, arXiv preprint arXiv:1804.02767, (2018).
- [23] N. Sajid, F. Faccio, L. Da Costa, T. Parr, J. Schmidhuber, and K. Friston, *Bayesian Brains and the Rényi Divergence*, Neural Computation, 34 (2022), pp. 829–855.
- [24] K. Simonyan and A. Zisserman, *Very Deep Convolutional Networks for Large-Scale Image Recognition*, in ICLR, 2015.
- [25] N. Srivastava, G. Hinton, A. Krizhevsky, I. Sutskever, and R. Salakhutdinov, *Dropout: A Simple Way to Prevent Neural Networks from Overfitting*, JMLR, 15 (2014), pp. 1929–1958.
- [26] C. Szegedy, S. Ioffe, V. Vanhoucke, and A. A. Alemi, *Inception-v4, inception-resnet and the impact of residual connections on learning*, in AAAI, 2017.
- [27] C. Szegedy, W. Liu, Y. Jia, P. Sermanet, S. Reed, D. Anguelov, D. Erhan, V. Vanhoucke, and A. Rabinovich, *Going deeper with convolutions. 2014*, arXiv preprint arXiv:1409.4842, 10 (2014).
- [28] M. Welling and Y. W. Teh, *Bayesian Learning via Stochastic Gradient Langevin Dynamics*, in ICML, 2011, pp. 681–688.
- [29] B. Wu, C. Xu, X. Dai, A. Wan, P. Zhang, Z. Yan, M. Tomizuka, J. Gonzalez, K. Keutzer, and P. Vajda, *Visual transformers: Token-based image representation and processing for computer vision*, arXiv preprint arXiv:2006.03677, (2020).
- [30] T. Yang, S. Zhu, C. Chen, S. Yan, M. Zhang, and A. Willis, *Mutualnet: Adaptive convnet via mutual learning from network width and resolution*, in ECCV, Springer, 2020, pp. 299–315.
- [31] H. Zhang, W. Liang, C. Li, Q. Xiong, H. Shi, L. Hu, and G. Li, *DCML: Deep Contrastive Mutual Learning for COVID-19 Recognition*, Biomedical Signal Processing and Control, 77 (2022), p. 103770.
- [32] T. Zhang, *From ϵ -entropy to KL-entropy: Analysis of minimum information complexity density estimation*, The Annals of Statistics, 34 (2006), pp. 2180–2210.
- [33] X. Zhang, J. Zhao, and Y. LeCun, *Character-level convolutional networks for text classification*, NeurIPS, 28 (2015).
- [34] Y. Zhang, T. Xiang, T. M. Hospedales, and H. Lu, *Deep Mutual Learning*, in CVPR, 2018, pp. 4320–4328.
- [35] H. Zhao, G. Yang, D. Wang, and H. Lu, *Deep Mutual Learning for Visual Object Tracking*, Pattern Recognition, 112 (2021), p. 107796.
- [36] J. Zhao, W. Luo, B. Chen, and A. Gilman, *Mutual-learning improves end-to-end speech translation*, in EMNLP, 2021, pp. 3989–3994.

Rényi Divergence Deep Mutual Learning: Supplemental Material

Weipeng Fuzzy Huang* Junjie Tao† Changbo Deng* Ming Fan† Wenqiang Wan*
 Qi Xiong* Guangyuan Piao‡

1 Simple and Straightforward Proofs of the Remarks

REMARK 1. For any distribution P , Q , and $\alpha \in [0, 1) \cup (1, \infty)$, the Rényi divergence $D_\alpha(P||Q) \geq 0$. The equality holds if and only if $P \equiv Q$.

Proof. The Rényi divergence has many forms. We transform the standard form to

$$\begin{aligned} D_\alpha(P||Q) &= \frac{1}{\alpha - 1} \log \int p(\mu)^\alpha q(\mu)^{1-\alpha} d\mu \\ &= \frac{1}{\alpha - 1} \log \int q(\mu) \left(\frac{p(\mu)}{q(\mu)} \right)^\alpha d\mu \\ &= \frac{1}{\alpha - 1} \log \mathbb{E}_q \left[\left(\frac{p(\mu)}{q(\mu)} \right)^\alpha \right] \end{aligned}$$

where $\mathbb{E}_q[\cdot] := \mathbb{E}_{\mu \sim q(\mu)}[\cdot]$ is the expectation operator over distribution Q with the corresponding density $q(\cdot)$, likewise for $\mathbb{E}_p[\cdot]$. As known, $f(x) = x^\alpha$ is convex in x for $\alpha > 0$. One can verify this through checking the second derivative of $f(x)$. Hence, given the Jensen's inequality,

$$\begin{aligned} D_\alpha(P||Q) &\geq \frac{1}{\alpha - 1} \log \left(\mathbb{E}_q \left[\frac{p(\mu)}{q(\mu)} \right] \right)^\alpha \\ &= \frac{\alpha}{\alpha - 1} \log \mathbb{E}_q \left[\frac{p(\mu)}{q(\mu)} \right] \\ &= \frac{\alpha}{\alpha - 1} \log \int p(\mu) d\mu = 0. \end{aligned}$$

Furthermore, the equality holds in Jensen's inequality almost surely when $p(\mu)/q(\mu)$ is constant. This concludes the proof. \square

REMARK 2. Given $\alpha \in [0, 1) \cup (1, \infty)$, the Rényi divergence $D_\alpha(P||Q)$ is non-decreasing in α , for any distribution P and Q .

Proof. Let us derive another form of the Rényi divergence, such that

$$\begin{aligned} D_\alpha(P||Q) &= \frac{1}{\alpha - 1} \log \int p(\mu)^\alpha q(\mu)^{1-\alpha} d\mu \\ &= \frac{1}{\alpha - 1} \log \int p(\mu) \left(\frac{p(\mu)}{q(\mu)} \right)^{1-\alpha} d\mu \\ &= \frac{1}{\alpha - 1} \log \mathbb{E}_p \left[\left(\frac{q(\mu)}{p(\mu)} \right)^{\alpha-1} \right]. \end{aligned}$$

Hence, we take the exponential of the Rényi divergence and acquire

$$\begin{aligned} \exp\{D_\alpha(P||Q)\} &= e^{\frac{1}{\alpha-1} \log \mathbb{E}_p \left[\left(\frac{q(\mu)}{p(\mu)} \right)^{\alpha-1} \right]} \\ &= e^{\log \left\{ \mathbb{E}_p \left[\left(\frac{q(\mu)}{p(\mu)} \right)^{\alpha-1} \right] \right\}^{\frac{1}{\alpha-1}}} \\ &= \left\{ \mathbb{E}_p \left[\left(\frac{q(\mu)}{p(\mu)} \right)^{\alpha-1} \right] \right\}^{\frac{1}{\alpha-1}}. \end{aligned}$$

It is assured that $q(\mu)/p(\mu) \geq 0$ when assuming all $p(\mu) > 0$. Based on the generalized mean inequality, for $\alpha' > \alpha$ (i.e., $\alpha' - 1 > \alpha - 1$), we achieve

$$\begin{aligned} \exp\{D_\alpha(P||Q)\} &= \left\{ \mathbb{E}_p \left[\left(\frac{q(\mu)}{p(\mu)} \right)^{\alpha-1} \right] \right\}^{\frac{1}{\alpha-1}} \\ &\leq \left\{ \mathbb{E}_p \left[\left(\frac{q(\mu)}{p(\mu)} \right)^{\alpha'-1} \right] \right\}^{\frac{1}{\alpha'-1}} = \exp\{D_{\alpha'}(P||Q)\} \end{aligned}$$

Since logarithm is monotonically increasing, we arrive at that $D_\alpha(P||Q) < D_{\alpha'}(P||Q)$ for $\alpha < \alpha'$ and $\alpha, \alpha' \neq 0$. \square

2 Additional Generalization Results

Since the generalization results for CIFAR100 and Flowers102 have been presented in the main text, we display the results for CIFAR10 and DTD here.

Vit for DTD is a clear case that RDML greatly improve the generalization performance over the original Vit model, for this task.

*Security Big Data Lab, Tencent Inc., China. {fuzzyhuang, changbodeng, johnnywan, keonxiong}@tencent.com

†School of Software Engineering, Xi'an Jiaotong University, China. taojunjie@stu.xjtu.edu.cn, mingfan@mail.xjtu.edu.cn

‡Department of Computer Science, Maynooth University, Ireland. guangyuan.piao@mu.ie

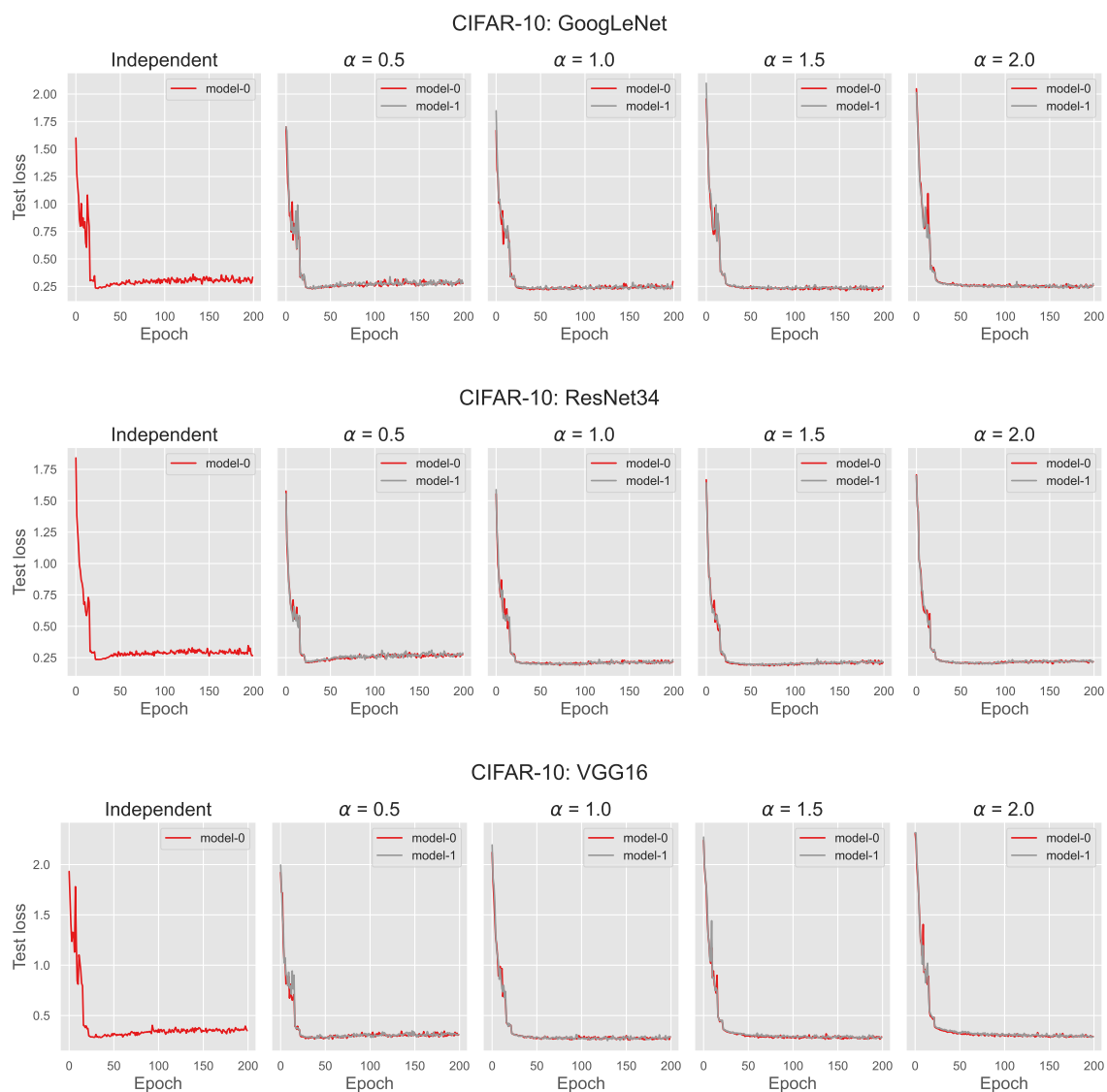


Figure S1: Test loss for the CIFAR10 dataset

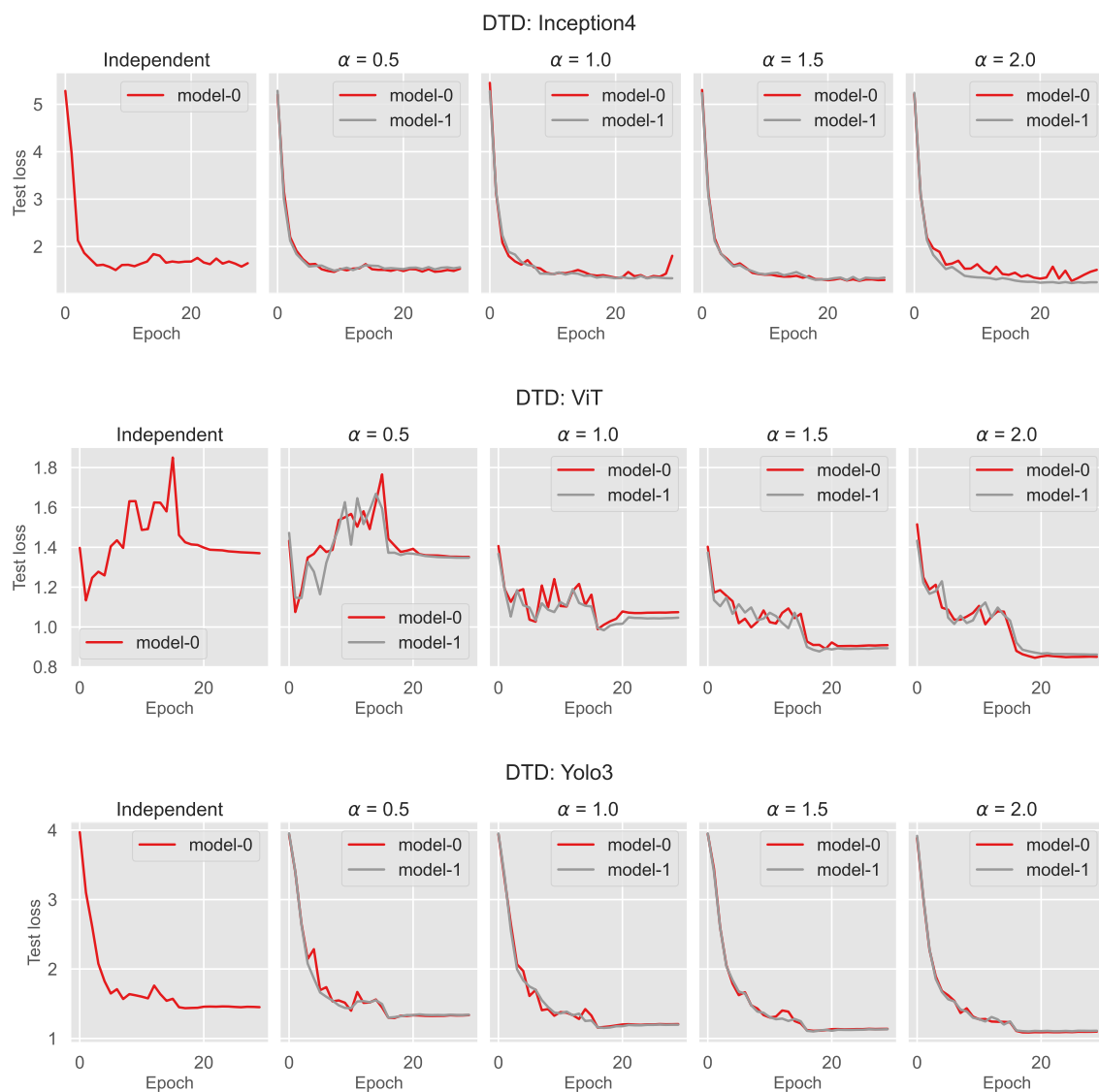


Figure S2: Test loss for the DTD dataset